Iranian Int. J. Sci. ***1****(2) 2000*

Deformational Behavior of Quartz and Feldspar in Quartzites within Shear Zones in the Adelaide Hills Area, South Australia

Ali Yassaghi,
Department of Geology, Tarbiet-Modaress University, Tehran, Iran
e-mail: yassaghi.SCI.TMU@net1cs.modares.ac.ir

Abstract

Observations on the deformational behavior of quartz and feldspar grains in the Stonyfell Quartzite within the shear zones in Adelaide Hills area show that quartz grains exhibit mainly intracrystalline deformation features while feldspar grains show mainly internal fracturing. In grains with greater dislocation density, however, quartz grains show evidence of dynamic recrystallisation and feldspar grains display only weak intracrystalline deformation features. From these observations it appears that strain and displacement along the shear zones was accommodated mainly by dislocation creep (crystal plastic) deformation mechanism. This can be constrain by the greater reduction in the lengths of short axes of quartz grains with respect to their long axes. Moreover, quantitative evaluation of the quartz-grain configuration data on a number of quartzite samples from within shear zones indicates that from the upper transitional zones toward the base of shear zones the grain size decreases, the aspect ratio increases, and the shape-preferred orientation of grains is modified due to shearing process. Similarly, the intensity of intracrystalline deformation features in quartz grains increases from the upper transitional zones towards the base of shear zones. Along the base of shear zones, softening mechanisms reduced the work-hardening process and increased the ductility of the quartzite which can be evidenced by the development of core and mantle structures.

Keywords: *Deformational behavior, quartzites, shear zones, South Australia*

1. Introduction

The microstructural development and deformation behavior of quartz (e.g. Bell & Etheridge 1973, White 1976, Voll 1976, Linker *et al*. 1984, Simpson 1985 and Hirth & Tullis 1992) and feldspar (e.g. Tullis & Yund 1985, 1987, and White & Mawer 1986) has been extensively studied in experimentally and naturally deformed quartzites. However, its deformation behavior is still not completely understood. This is because quartz is a sensitive indicator of variations of strain orientation and intensity as well as of the rate controlling deformation mechanisms operating (e.g. Etheridge & Wilkie 1979, and O'Hara 1988 & 1990). The deformational behavior of feldspar is also strongly dependent on metamorphic (i.e. pressure and temperature) conditions (e.g. Tullis & Yund 1991, and Pryer 1993).

The study of microstructures in shear zones provides with information regarding the variations of grain scale microstructures (e.g. Passchier & Trouw, 1995), the environmental conditions of deformation (e.g. Boullier 1980, and Hirth & Tullis 1992), and the deformation history (e.g. Schmid 1982, and Tullis *et al*. 1982). In this paper, microstructural development and deformational behavior of individual grains of quartz and feldspar is examined in selected samples of the Stonyfell Quartzite units from weakly deformed rocks outside and/or in the upper transitional zones to more deformed rocks near the lower boundary thrust which makes the base to the shear zones. The aim of this manuscript is to investigate the deformation processes operating in the quartzites within the shear zones which affected mainly on grain-scale microstructural changes, and to determine deformation mechanisms acting on the shear zones.

2. Geological setting of the Adelaide Hills area

The Adelaide Hills area is situated east of Adelaide city and is a part of the southern Mt. Lofty Ranges in northern part of the Southern Adelaide Fold-Thrust Belt. In the area, a number of discrete early proterozoic basement inliers are overlain by a sequence of late Precambrian Adelaidean metasedimentary rocks, which are broadly recognized as clastic sediments of the Burra Group (Preiss, 1987). The Burra Group in this area, based on previously published geological maps (Forbes 1980, 1983), mainly comprises multiple units of competent quartzite of the Aldegate Sandstone and Stonyfell Quartzite Formation interleaved with incompetent pelitic and phyllite rocks of the Woolshed Flat and Saddleworth Formations, and is overlying the basement inliers (Fig. 1). Detailed structural mapping along the few accessible roads (as the area mainly covered by vegetation and housing), reveal six major stacked parallel shear zones with generally NE-SW trends and shallow SE dips which has been named as the Morialta, Greenhill-Montacute Heights, Norton Summit, Pole Road-Summertown, Clarendon, and Mt. Bold shear zones from NW to SE, respectively (Yassaghi *et al.* 1995) (Fig. 1). These shear zones are spatially concentrated zones of deformation, including an array of fabrics and minor structures. These fabrics and structures are incipiently developed at the upper transitional zones to the shear zones and moderately developed within the shear zones. They are strongest along the base of the shear zones (Yassaghi 1998).

3. Study objectives

A study of quartzite microstructures has been carried out on 11 samples of quartzofeldespathic rocks of the Stonyfell Quartzite, along the structural transects from outside towards the base of the shear zones. For convenience of the description microstructures of the samples is divided into three groups based upon the different characteristics (sub-zones I, II, and III). A sketch of the typical location of each sub-zone from within the shear zones is shown in Figure 2. As can be seen, sub-zone I is in the upper transitional and/or outside the shear zones but approaching the margins of the shear zones. Sub-zone II is in the middle part of the shear zones, and sub-zone III is closer to, or at the base of the shear zones. Oriented specimens were collected from each sub-zones and cut parallel to the stretching lineation and perpendicular to cleavage (the XZ plane of the local finite strain). Because of similarities of microstructures from the different shear zones, only one of the shear zones (Pole Road shear zones, Fig. 1) which have the best outcrops are presented and discussed in more detail here. Some detailed microstructural description of the other shear zones is also tabulated in Table 1.

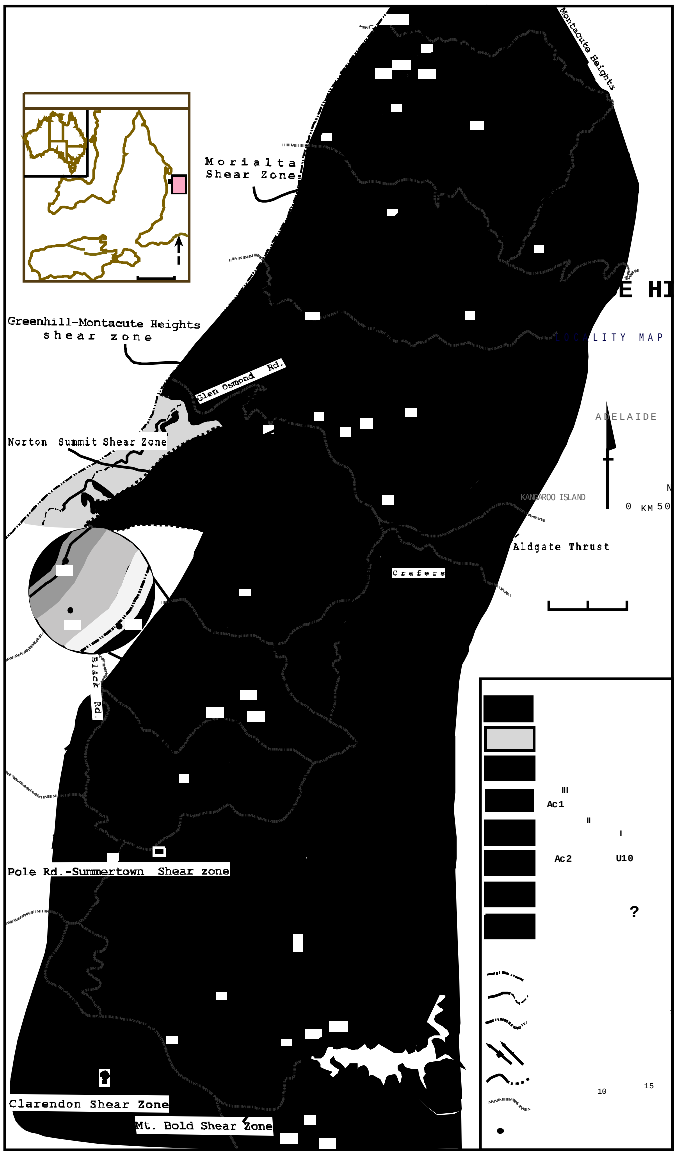

Figure 1 - Geological map of the Adelaide Hills area showing the location of shear zones and associated thrusts. Map is compiled from data of geological survey mapping (Forbes 1980, 1983) and from mapping by Yassaghi (1998). Circle shows a sketch of the sub zones location in the Pole Road shear zone.

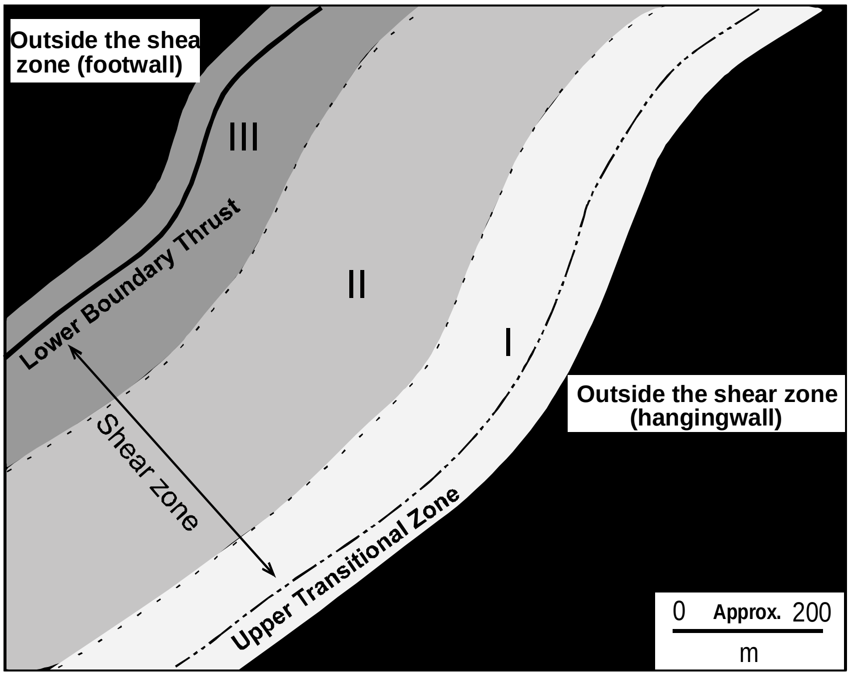

Figure 2 - Sketch showing general location of sub-zones in the shear zones; sub-zone I covers the upper transitional zones/outside shear zones, sub-zone II is located within shear zones, and sub-zones III covers the areas around the lower boundary thrusts. The location of this sketch for the Pole Road shear zone is also shown in Figure 1.

4. Microstructures of quartz and feldspar in the shear zones

The modal analyses of the samples from the three sub-zones resulted in quartz (~85%), feldspar (~15%) and very small amounts of white mica (~0.5 %). The sample collected from the sub-zone II was located about 200m from the sample collected from the sub-zone I, and about 100m from the sample collected from the sub-zone III. Detailed microstructures of each sample are described individually as follows:

In a sample from Sub-zone I, quartz grains are almost equant polygonal (with 790 m mean grain size) and slightly elongate with lobate and serrated grain boundaries. The grains exhibit intracrystalline deformation features such as patchy to slightly undulatory extinction and grain boundary serration in which small (~20 m) white mica grains are located. Evidence of recovery in the form of deformation bands is also seen in grains with higher dislocation density (Fig. 3a). The characteristics of quartz microstructures are similar to experimentally deformed quartz developed at the first stage of shearing (Simpson 1994) or in regime one of Hirth and Tullis (1992). Feldspar grains consist of plagioclase (mostly albite) and potassium feldspar (mostly microcline and orthoclase) with approximately the same grain size as the quartz grains. They are almost all fractured and partly alteared to white mica or zoisite (see bottom right corner of Fig. 3a). They also show weak undulatory extinction.

In a sample from sub-zone II, the quartz grains have a mean grain size of 670 m and are more elongate than those of sub-zone I, and their grain boundaries are sutured. They show intracrystalline deformation features such as sweeping undulatory extinction, deformation bands and subgrain structures (Fig. 3b). Evidence of minor grain boundary migration and recrystallised small grains are also seen around the boundaries of the grains which have greater dislocation density. This type of microstructure is similar to the microstructures developed in regime two of the experimentally deformed quartzites of Hirth and Tullis (1992), in which a subgrain rotation microstructure is suggested to be responsible for recovery at moderate temperatures or slow strain rates (Urai *et al*. 1986, Hirth and Tullis 1992, and Simpson 1994). Feldspar grains as in sub-zone I show slightly undulatory extinction and intracrystalline fractures (middle right side of Fig. 3b). Some feldspars show offset along these fractures.

In a sample from sub-zone III, the mean grain size is 590 m and grains are more equant unlike sub-zone II. Two main microstructural changes of the quartz grains from sub-zone II are observed. They are: (i) an increase in the amount of sweeping undulatory extinction and deformation bands, and (ii) an increase in the frequency of recrystallised small grains on the margins of original grains, which show the initiation of core and mantle structure (White 1976) (Fig. 3c). These microstructures are almost identical to microstructures developed in regime three of Hirth and Tullis (1992) in experimentally deformed quartzites in which dislocation climb is sufficiently high to control recovery at high temperature or lower strain rate.

The feldspar grains in sub-zone III are almost all fractured and typically display extension and shear fractures, which result in the production of angular and elongate fragments. The feldspar grains as shown in Figure 3d are split into elongate tabular fragments which have their upper halves offset to the left with respect to their lower halves along synthetic low-angle normal microfractures (Pryer 1993, and Simpson 1994). These microstructures indicate overall top to the NW sense of shear movement for the Pole Road shear zone.

The detailed study of microstructures from the Stonyfell Quartzite adjacent to and within the shear zones show that the amount of deformation increases from sub-zone I to sub-zone III (see also Table 1 for comparison). This change in deformational behavior is more evident in quartz grains while the feldspar grains almost all display intracrystalline fracturing.

Figure 3 - Photographs of minor structures and photomicrographs of microstructures. (a), (b), (c), and (d) are crossed polars and width of view in (a), (b), (c) is 2.5 mm but in (d) is 1.2 mm. Thin sections cut parallel to the stretching lineations and perpendicular to cleavage. (a): Slightly deformed quartzite from sub-zone I. Note weak intracrystalline deformation and grain boundary bulge. (b): More deformed quartzite from sub-zone II. Note greater development of intracrystalline features like deformation bands (DB) and subgrains (SG). (c): More highly deformed quartz from sub-zone III. Note widespread development of recrystallised small grains at the margin of original grains. (d): Displaced broken feldspar in quartzite from within the Mt. Bold shear zone; note that the feldspar is displaced along a microshear parallel to the mesoscopic shear plane and indicates NW (to the left) sense of displacement. (e): Asymmetric boudinaged quartz veins from within the Mt. Bold shear zone; from the asymmetric tails of the boudins the sense of movement can also be defined which is towards right. (f): Development of en-echelon quartz veins in the Stonyfell Quartzite within the Morialta shear zone; note that the veins were deformed progressively in a semi-ductile manner in which more than one generation of the veins can be seen.

Microstructural comparison of quartz and feldspar in quartzites from the Mt. Bold toward the Morialta shear zones (Table 1) shows that the core and mantle structure in the Morialta shear zone is achieved by greater subgrain rotation recrystallisation than in the Mt. Bold shear zone. Similarly, general evidence of solution mass-transfer deformation mechanisms such as beards containing white mica and small quartz grains is also seen in the Morialta shear zone. Feldspar grains show increasing amounts of intracrystalline fractures toward the Mt. Bold shear zone in which the margins of feldspars are displaced to produce bookshelf structures (Passchier 1982, Pryer 1993) (for example see Fig. 3d).

5. Quantitative microstructural analysis of quartz grains

A study of the variation of grain size, grain shape (aspect ratio) and shape preferred orientation (ø) has been made to demonstrate and tentatively quantify development of microstructures (Figs. 4 & 5). The comparison of these parameters has also been performed across the Mt. Bold, the Pole Road, and the Morialta shear zones to integrate the results with these microstructural analyses. Measurement of the parameters was carried out on enlarged photomicrographs which were taken from the oriented (XZ) thin sections. A minimum of 40 measurements of the parameters were digitized from each sample using the numerical software package DIGITIZE (RockWare, Inc. 1989).

5.1 Grain size analysis

The histograms of log grain size (Fig. 4) show the distributions of the values of mean and median grain size of each sample across the shear zones. In almost all the shear zones this value decreases from sub-zone I to sub-zone III. It can also be seen that there is a general trend of decrease in grain size from the Mt. Bold toward the Morialta shear zones (see also Table 1).

Scatter graphs of long axis versus short axis length for each sub-zone were constructed and their regression lines and R^2 (the goodness-of-fit statistic which is often used to convey the quality of a regression line) were also calculated (Fig. 4). These graphs demonstrate: (1) the distribution and proportion of grain size reduction between larger and smaller detrital grains and (2) the variation in distribution of long axis and short axis. As can be seen in Figure 4, across all the shear zones from sub-zone I to sub-zone II, the larger grains appear to undergo greater grain size reduction than the smaller ones. For instance, in the Pole Road shear zone, from sub-zone I to sub-zone II the values of log-long axis (L) and log-short axis (W) of most of the larger grains is reduced (by about 10% in size), while of the smaller grains remain constant. Continuing to sub-zone III, however, the size of the smaller grains is also decreased (by about 15% in size) (e.g. see the graphs of the Morialta shear zone in Fig. 4).

Similarly, the range of distribution of the values of long axis versus short axis lengths from sub-zone I to sub-zone III across most of the shear zones varies systematically. This can be demonstrated by a decrease in the value of “b” (gives the gradient of the regression line) and an increase in the value of “a” (gives the intercept of the regression line on the y axis) in the calculated and constructed regression line functions ($Y=bX + a$, the equation of the best fit regression line), which cause a decrease in the slope of the regression lines. For example, in samples from Pole Road shear zone (Fig. 4) the value of “b” decrease from 0.8801 in sub-zone I to 0.6286 in sub-zone III. Considering reduction of the grain size across the shear zones from sub-zone I to sub-zone III, the decrease in the slope of the trend lines implies that the values of short axes decreases more than the values of the long axes.

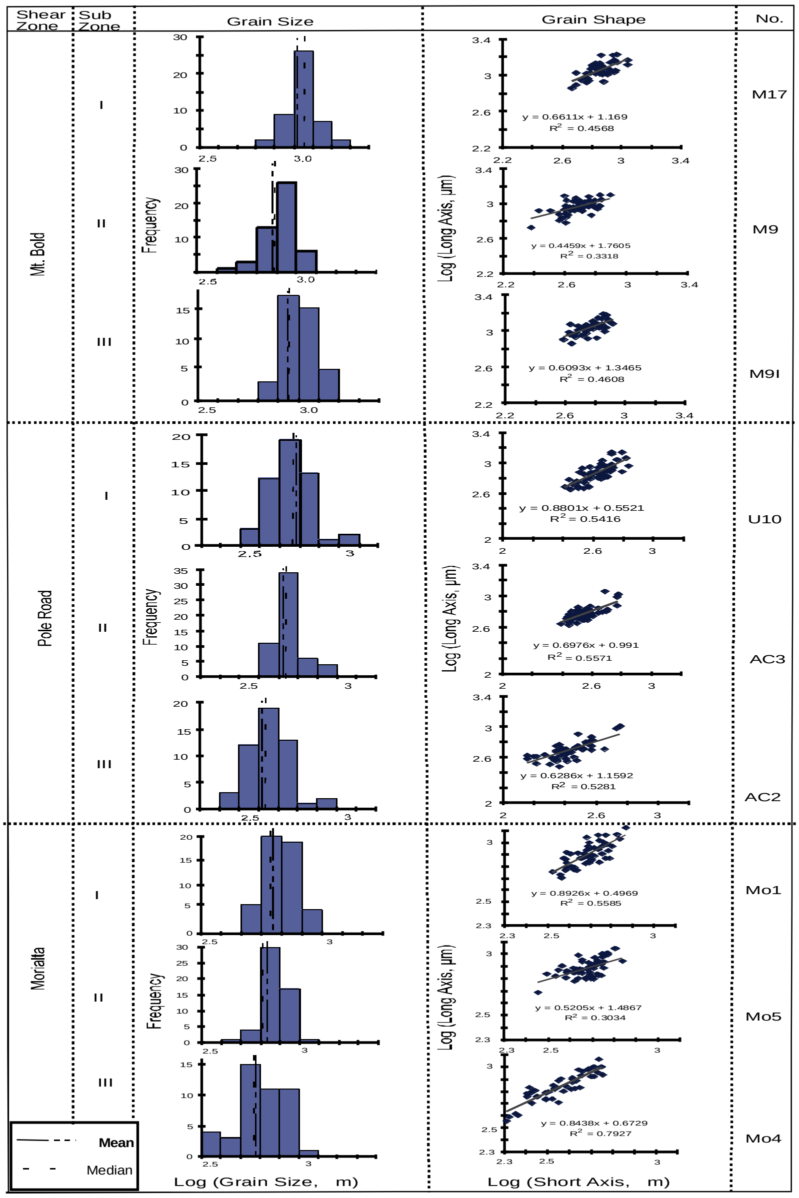

Figure 4 - Distribution of grain size and grain shapes of the quartzites. Note decrease in the mean value of grain size from the transitional zones (sub-zones I) toward the base of the shear zones (sub-zones III).

5.2 Grain shape (aspect ratio) analysis

The grain shape distributions (Fig. 5) show that the aspect ratio of grains increases from sub-zone I to sub-zone III in each shear zone and all samples have an average ranging from 1.6 to 2.0. It also shows that this average of the sub-zone III of all the shear zones is almost constant. The slightly higher value in samples from sub-zone I (e.g. the Mt. Bold shear zone) may be due either to regional deformation or to a shape effect of the original grains due to synsedimentary compaction.

5.3 Shape-preferred orientation (Ø) analysis

The histograms of Figure 5 display the distribution of the values of Ø (the angle between long axes of grains and the reference frame) across the shear zones. These values in all samples were measured with respect to bedding. As can be seen in Figure 5, there is a variation in the degree of shape-preferred orientation from sub-zone I to III. Long axis orientation of the grains in most samples (e.g. samples from the Pole Road shear zone and especially the ones from sub-zone III) show a distribution about the plane of the tectonic fabric. However, samples with a weak long axis orientation about the plane of tectonic fabric may be interpreted as: (a) representing a pre-existing sedimentary fabric (# M17, Fig. 5) or (b) recording a slightly greater intensity of deformation (possibly # M9I, Fig. 5) or (c) a combination of both of the above (probably # H9, Fig. 5).

6. Discussion

6.1. Microstructural development within quartzites in the shear zones

The microstructural development of each shear zone from the transitional zone to the basal thrust, that is from sub-zone I to sub-zone III, shows that the dynamic recrystallisation process is likely to be the dominant process in the development of the shear zones. The accumulation of dynamic recovery products such as grain boundary migration recrystallisation (GBMR) and sub-grain rotation recrystallisation (SRR) at the base of the shear zones demonstrates that toward these boundaries, the temperature increases or the strain rate decreases (Hirth & Tullis 1992, Lloyd & Freeman 1994). Similarly, an increase in the relative proportion of SRR to GBMR towards the Morialta shear zone also shows that toward this shear zone the temperature becomes moderate to low or strain rate increase (e.g. Hirth & Tullis 1992 and Kirschner *et al.* 1995). This therefore is further supporting evidence that temperature decreases or strain rate increases within the shear zones closer to the foreland relative to those closer to the hinterland.

6.2. Environment conditions and deformation mechanisms of the shear zones

It has been shown that feldspar in the shear zones deformed consistently by cataclasis with fragments separated by mica flakes (for example Fig. 3d). No evidence for subgrain development, deformation twinning or recrystallisation along grain boundaries or cracks was found. This suggests that within feldspars crystal plastic processes were not substantially active and deformation temperatures were below 450 °C (e.g. Tullis 1983, Simpson 1985, O'Hara 1990, and Bailey *et al.* 1994). The parallelism of the mica flakes to syntectonic fractures or microshears in feldspars (Fig. 3d) suggests that feldspar dissolution with concurrent reaction to form white mica occurred along these movement planes.

Quartz grains in the shear zones on the other hand are obviously deformed and exhibit overwhelming evidence of crystal plastic deformation mechanisms, such as sweeping undulatory extinction, deformation bands, subgrain formation and core and mantle structure. These microstructures indicate that rotational recrystallisation is more active than dislocation glide. Crystal plastic deformation becomes effective in quartz at temperatures near 300°C, whereas lack of complete recovery suggests deformation temperatures within the greenschist facies (e.g. Voll 1976, Simpson 1983, 1985, and Bailey *et al.* 1994). Since there is no extensive evidence of quartz ribbon grains, deformation in the shear zones is most likely to have occurred at lower greenschist facies (e.g. Simpson 1985, and Bailey *et al.* 1994).

The above considerations suggest that deformation took place between 350-450°C. From the Mt. Bold shear zone toward the

Morialta shear zone the amounts of intracrystalline fracture of feldspar, and deformation bands and core and mantle structure of quartz decreases, while the amount of dissolution products such as corrosion of quartz grains and beards of small quartz and mica increases. An increase in the amount of dynamic recovery products is expected at higher temperatures or slower strain rates, since recovery involves the thermally activated climb of dislocations. Therefore, a decrease in the amount of crystal plastic deformation products toward the Morialta shear zone might possibly be due to a decrease in the temperature or an increase in fluid activity (Simpson 1985) toward the NW. These microstructures are recognised to occur in association with conditions of brittle-ductile transition (Simpson 1985, and Bailey *et al.* 1994).

The semi-brittle nature of the deformation would facilitate significant amounts of dissolution in feldspar and quartz. A substantial increase in the amount of dissolution in quartz and to a lesser extent in feldspar from the Pole Road shear zone toward the Morialta shear zone further constrains the transitional nature of deformation from ductile to brittle-ductile across the shear zones. Such a transition from ductile to brittle-ductile deformation can also be seen in quartz veins across the shear zones. In the Mt. Bold shear zone, almost all quartz veins are deformed by ductile deformation to produce folded and boudinaged veins (Fig. 3e), while in the Morialta shear zone the quartz veins are deformed by semi-ductile deformation to produce en-echelon tension gash structures (Fig. 3f). This transition in the formation of quartz veins across the shear zones provides further support that the brittle-ductile transition conditions of deformation were prevalent in the shear zones.

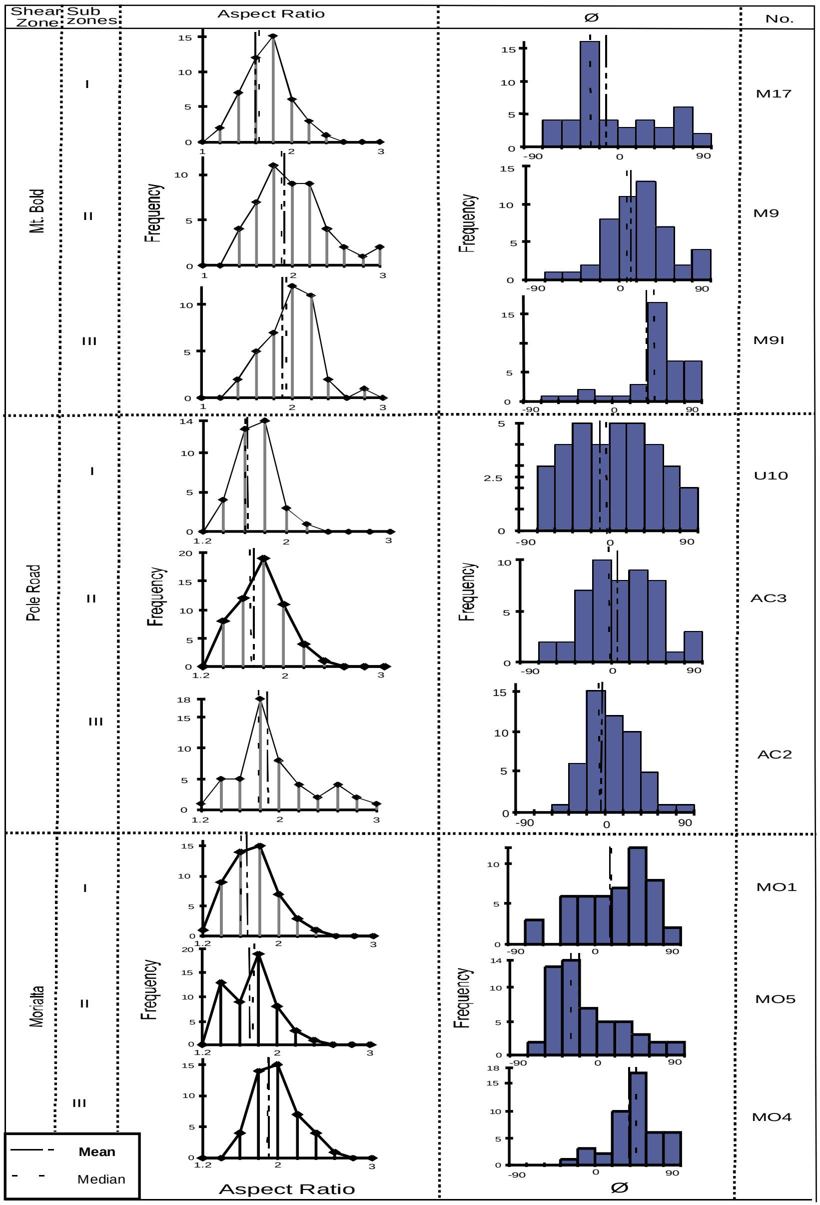

Figure 5 - Aspect ratio and shape-preferred orientation of grains within quartzites.

6.3. interpretation of the quartz-grain configuration data

Grain size is an important variable in fault zone deformation and formation of fault rocks in shear zones and generally involves a reduction in grain size (White 1979, Etheridge & Wilkie 1979, Newman & Mitra 1993, Michibayashi 1996). Quantitative analysis of the grain size distributions from sub-zone I toward III, i.e., from the upper transitional zone toward the base of shear zones, in almost all the shear zones, show a substantial reduction in grain size (Fig. 4). It is widely accepted that such reduction might be due to the development of microstructures involving increase in shear strain during dynamic recovery and/ or recrystallisation (Bell & Etheridge 1976, White 1973, 1976, 1977, Etheridge & Wilkie 1979, Evans & White 1984, and Newman & Mitra 1993).

The proportion of reduction in grain size is not equally partitioned between larger and smaller grains. As can be seen on scatter graphs of Figure 4, from sub-zone I to II, the sizes of the larger grains are reduced while the smaller ones remain almost unchanged. The progression to sub-zone III, however shows that the amount of ductile deformation increases, and all grains are reduced in size. It is assumed that microfracturing, without significant dilation, is the initial deformation mechanism of the shear zone development (Knipe & White 1979). Such fracturing can be seen mostly in samples from sub-zone I. This fracturing is considered to be responsible for grain size reduction of original detrital grains in sub-zone II prior to dynamic recovery and/or recrystallisation, a process which occurred mainly at the base of the shear zones or in sub-zones III.

A marked reduction in grain size is also observed from the Mt. Bold shear zone toward the Morialta shear zone (Fig. 4 and Table 1). This reduction might not only be due to an increase in the amount of shear strain or ductile deformation but also, more likely, because of the presence of phyllosilicate minerals, many of which grow by processes of solution mass-transfer. Taking into account the qualitative study of microstructures of the shear zones (see Table 1 for more detail), it now can be ascertained that in the Mt. Bold and Norton Summit shear zones, the grain size reduction is more likely due only to crystal plastic deformation mechanisms but in the Pole Road and Morialta shear zones further reduction of grain size might be due to both crystal plastic and solution mass-transfer deformation mechanisms. These shear zones are thought to have been generated at higher crustal levels, possibly during their imbrication and emplacement as described elsewhere, for example, by Evans and White (1984).

Variations in the range of distribution of the values of long axes versus short axes across almost all of the shear zones shows that toward sub-zone III the values of the lengths of the short axes decrease more than the elongation of long axes. This can be seen by decreases in the values of “b” and increases in the values of “a” in the trend-line functions (Fig. 4) across each shear zone. Similarly, the proportion of the aspect ratio between the larger grains and smaller ones is not constant and it is the smaller grains which show mostly higher aspect ratios. This is in accordance with the observation that smaller grains are affected more by the processes of dynamic recovery and recrystallisation during shear zone development. This is because crystal plastic processes produce elongate grain shapes with higher aspect ratios (Passchier & Trouw 1995). The results of the quantitative analyses also show that there is a positive correlation between the increase in aspect ratio of grains and the development of shape-preferred orientations.

7. Conclusion

Detailed studies of quartz microstructures in quartzites across the shear zones show that in samples from outside the zones, quartz grains exhibit mainly intracrystalline deformation such as undulatory extinction. Within the shear zones, however, they show evidence of shear bands, subgrains, and core and mantle structures in grains with greater dislocation densities. These microstructures exhibit overwhelming evidence of crystal-plastic deformation mechanisms across the shear zones. Based on the decrease in intensity and development of the core and mantle structures, the amount of this deformation mechanism decreases from the shear zones closer to the hinterland towards those on the foreland side where evidence of pressure solution deformation mechanisms were seen in impure quartzites.

Quantitative analyses of quartz-grain configuration show that all quartz grains are reduced in size during the shear zone development. Crystal-plastic deformation mechanisms are considered to be responsible for this reduction. Further reduction of quartz grains in samples from the foreland-side shear zones is recognized to be due to both the effects of crystal plastic and pressure solution deformation mechanisms. Similarly, the analyses confirm that within the shear zones the aspect ratios of the quartz grains increase, and their shape-preferred orientations also change. These reorganisation of quartz grain configurations within the shear zones are considered to be due to shearing process.

Acknowledgment
This study is a part of the author's PhD funded by a scholarship from the Ministry of Culture and Higher Education of the Islamic Republic of Iran for which he is most grateful. Sincere thanks are due to Dr. Patrik R. James and Dr. Thomas Flottmann for their friendly suggestions and advice.

References

Bailey, C.M., Simpson, C., and De Paor, D.G., (1994) *Volume loss and tectonic flattening strain in granitic mylonites from the Blue Ridge province, central Appalachians*. Journal of Structural Geology **16,** 1403-1416.

Bell, T.H., and Etheridge, M.A., (1973*) Microstructure of mylonites and their descriptive terminology*. Lithos **6,** 337-348.

Boullier, A.M., (1980) *A preliminary study on the behaviour of brittle minerals in a ductile matrix; example of zircons and feldspars*. Journal of Structural Geology **2**, 1/2, 211-217.

DIGITIZE (1989) Digitizing softwear for macintosh, RockWare, Inc.

Etheridge, M. A. and Wilkie, J. C. (1979) Grain size reduction, grain boundary sliding and the flow strength of mylonites. *Tectonophysics* **58** 159-178.

Evans, D.J., and White, S.H., (1984) *Microstructural and fabric studies from the rocks of the Moine Nappe, Eriboll, NW Scotland*. Journal of Structural Geology **6** (4), 369-389.

Hirth, G., and Tullis, J., (1992) Dislocation creep regimes in quartz aggregates. *Journal of Structural Geology* **14** (2), 145-159.

Kirschner, D.L., Teyssier, C., Gregory, R.T., (1995) *Effect of deformation on oxygen isotope exchange in the Heavitree Quartzite, Ruby Gap duplex, central Australia*. Journal of Structural Geology **17** 1407-1423.

Knipe, R.J., and White, S.H., (1979) *Deformation in low grade shear zones in the Old Red Sandstone, S.W. Wales*. Journal of Structural Geology **1** (1), 53-66.

Linker, M.F., Kirby, S.H., and Alison O., (1984) *Effects of compression direction on the plasticity and rheology of hydrolytically weakened synthetic quartz crystals at atmospheric pressure*. Journal of Geophysical Research.

Lloyd, G.E., and Freeman, B., (1994) *Dynamic recrystallization of quartz under greenschist conditions.* Journal of Structural Geology **16,** 867-881.

Michibayashi, K., (1996) *The role of intragranular fracturing on grain size reduction in feldspar during mylonitization*. Journal of Structural Geology **18,** 1-17.

Newman, J., and Mitra, G., (1993) *Lateral variations in mylonite zone thickness as influenced by fluid-rock interactions, Linville Falls Fault, North Carolina*. Journal of Structural Geology **15**, 7, 849-863.

O'Hara, K,. (1988) *Fluid flow and volume loss during mylonitization; an origin for phyllonite in an overthrust setting, North Carolina, U.S.A.* Tectonophysics **156,** (1-2), 21-36.

O'Hara, K., (1990) *State of strain in mylonites from the western Blue Ridge Province, Southern Appalachians; the role of volume loss.* Journal of Structural Geology **12** (4), 419-430.

Passchier, C.W., (1982) *Pseudotachylyte and the development of ultramylonite bands in the Saint-Barthelemy Massif, French Pyrenees*. Journal of Structural Geology **4** 1, 69-79.

Passchier, C.W., and Trouw, R.A.J., (1995) Microtectonics. Springer, 289.

Preiss, W.V., (1987) The *Adelaide Geosyncline - late Proterozoic stratigraphy, sedimentation, palaeontology and tectonics*. Geol. Survey S. Aust. Bull. **53** 1-438.

Pryer, L.L., (1993) *Microstructures in feldspars from a major crustal thrust zone; the Grenville Front, Ontario, Canada.* Journal of Structural Geology **15** 1, 21-36.

Schmid, S.M., (1982) *Microfabric studies as indicators of deformation mechanisms and flow laws operative in mountain building. 95-110*

Simpson, C. (1985) Deformation of granitic rocks across the brittle-ductile transition. Journal of Structural Geology **7** (5), 503-511.

Simpson, C., (1994). 100 photomicrographs of microstructures, Earth'nWare Inc. & Industrial Association of George Washington Uni.**:** 27.

Tullis, J., (1983) *Deformation of feldspars. Feldspar mineralogy. P. H. Ribbe. Mineral.* Soc. Am. Rev. Mineral., **2:** 297-323.

Tullis, J., Snoke, A. W. and Todd, V. R. (1982) *Significance and petrogenesis of mylonitic rocks*. Geology **10,** 227-230.

Tullis, J., and Yund, R.A,. (1985) *Dynamic recrystallization of feldspar; a mechanism for ductile shear zone formation*. Geology (Boulder) **13**, 4, 238-241.

Tullis, J., and Yund, R.A., (1991) *Diffuse creep in feldspar aggregates; experimental evidence.* Journal of Structural Geology **13**, 9, 987-1000.

Urai, L., Means, W., & Lister, G., (1986*) Dynamic recrystallisation of minerals.* Geophysical Monograph **36** 161-199.

Voll, G., (1976) *Recrystallization of Quartz, Biotite and Feldspars from Erstfeld to the Leventina Nappe, Swiss Alps, and its* *geological significance*. Schweiz. mineral. petrogr. *Mitt.* **56** 641-647.

White, J.C., and Mawer, C.K., (1986) *Extreme ductility of feldspars from a mylonite, Parry Sound, Canada.* Journal of Structural Geology **8** 2, 133-143.

White, J.C., and White, S.H., (1983*) Semi-brittle deformation within the Alpine fault zone, New Zealand.* Journal of Structural Geology **5** 6, 579-589.

White, S., (1973) *Syntectonic Recrystallization and Texture Development in Quartz*. Nature (London*)* **244** 5414, 276-278.

White, S., (1976) *The effects of strain on the microstructures, fabrics, and deformation mechanisms in quartzites*. Philosophical Transactions of the Royal Society of London, Series *A: Mathematical and Physical Sciences* 283; 1312, A discussion on natural strain and geological structure, 69-86.

White, S., (1977) *Geological significance of recovery and recrystallization processes in quartz*. Tectonophysics **39** 1-3, 143-170.

White, S., (1979) *Grain and sub-grain size variation across a mylonite zone*. Contrib. Mineral. Petrol. **70,** 193-202.

White, S.H., Bretan, P. G. and Rutter, E. H. (1986*) Fault-zone reactivation: kinematics and mechanisms*. Phil. Tran. R. Soc. Lond. **A317,** 81-97.

Yassaghi, A., (1998) *Geometry, kinematics, strain analysis, and P-T conditions of shear zones in Adelaide Hills area*. PhD. Dese. Adelaide Uni. South Australia.

Yassaghi, A., James, R.P., Flottmann, T. (1995) *Some constraints on geometrical evolution of ductile thrusts and shear zones in Adelaide Hills area*. SGTSG Clare valley Conference, Australia, 180-181.

Table 1: General description of microstructures of quartz and feldspar in quartzites. Labels; Qtz: qua bands, GBMR: grain boundary migration recrystallisation, SRR: subgrain rotation recrystallisation, S sweeping undulatory extinction, and SMT: solution mass-transfer. I, II, and III are sub-zones of the sh

Shear Zones	Specimens & Sub-zones	Main Mineralogy	Grain Size (?m) Qtz & F	Mica	Micr Quartz
Mt. Bold	M17 (**I**)	Quartz (~85%), Feldspar (~15%) & White Mica (~0.5%)	890	~20	Patchy to slight undulatory extinction and grain boundary bulging
	M9 (**II**)	Quartz (~85%), Feldspar (~15%) & White Mica (~0.5%)	680	~20	SUE, DB, SS and GBMR in grains with greater dislocation densities
	M9I (**III**)	Quartz (~85%), Feldspar (~15%) & White Mica (~0.5%)	790	~20	Increase in the amount of SUE, DB, SS and more evidence of GBMR and in some grains SRR to develop core & mantle structure
	M11 (**II**)	Quartz (~90%), Feldspar (~10%) & White Mica (~0.5%)	870	~20	SUE, DB, SS and development of grain boundary bulging at the margin of some grains which show initiation of GBMR
	M36 (**III**)	Quartz (~90%), Feldspar (~10%) & White Mica (~0.5%)	820	~20	SUE, DB, SS, more evidence of GBMR than sub-zone II and in some grains SRR to develop core & mantle structure
Pole Road	U10 (**I**) Fig. 3a	Quartz (85-90%), Feldspar (~10-15%) & White Mica (~1%)	570	~30	Random extinction but in some grains slight undulatory extinction & SS
	AC3 (**II**) Fig. 3b	Quartz (85-90%), Feldspar (~10-15%) & White Mica (1-2%)	480	~50	Slightly SUE, DB, SS and on grains with more dislocation density SRR
	AC2 (**III**) Fig. 3c	Quartz (85-90%), Feldspar (~10-15%) & White Mica (~2%)	440	~200	SUE, DB, SS. Grain boundaries of some grains are sutured to produce SRR and/or with less developed GBMR or are truncated by white mica
Morialta	MO1 (**I**)	Quartz (~85%), Feldspar (~10%) & White Mica (~5%)	640	~100	Patchy to slight UE, DB in some grains. Grain boundary serration & bulging and growth of small white mica on the margin of grains
	MO5 (**II**)	Quartz (~80-85%), Feldspar (~10%) & White Mica (5-10%)	600	100-300	Patchy to slight UE, DB & SS in some grains. Grain boundaries are truncated by flakes of mica. Some grains show beards of small quartz & mica
	MO4 (**III**)	Quartz (~80%), Feldspar (~10%) & White Mica (~10%)	500	~400	Large evidence of SMT such as beards of small quartz & mica, corrosion and truncation of grains by large mica. On some original grains SUE, SS, DB & recrystallised small grains due to SRR